DOI: 10.58895/ksp/1000150865 -4 erschienen in:
Forum Bildverarbeitung 2022 | Image Pocessing Forum 2022
DOI: 10.5445/KSP/1000150865 | https://www.ksp.kit.edu/site/books/m/10.58895/ksp/1000150865/

Blurred resolution enhancement by graphene nanoplates

Laura Carrilero[1], José R. Castro[1], Sandra Pérez[1], Tomás Belenguer[2], and Félix Salazar[1]

[1] ETSIME (UPM),
C/ Ríos Rosas 21, 28003 Madrid
[2] LINES (INTA),
Torrejón de Ardoz, 28850 Madrid

Abstract Imaging through turbid media leads to a great loss of information decreasing the image quality. In this work we try to palliate this problem by adding an absorbent to the medium, eliminating part of the scattered radiation responsible for the turbidity. This research work is preceded by the demonstration of the effectiveness of black carbon powder as an absorbent, leading to improved quality images [1,2]. With this aim, we use graphene nanoplates as an absorbent and compare the results with black carbon powder in order to study the possible improvement.

Keywords Vision, absorption, scattering, turbid media

1 Introduction

When a medium is interposed between an object and the detection system, there is a loss of quality of the transmitted image due to the light behavior through the medium. The transparency property of a system affects how the light behaves passing through it. For instance, translucent materials, such as diffusive media, allow light to pass through them, but it suffers changes. Some photons pass through the body and reach the detector without alterations (ballistic photons), some fail to pass through it and are retained in the medium (absorbed photons) and others suffers changes in its trajectory (scattered photons), not allowing a clear vision, since they arrive the detector in a random manner. Adding an absorber to the medium can improve the image quality

since it has more chances to absorb the scattered photons due to its longer path than the ballistic ones, hence part of the scattered radiation will be eliminated before reaching the detector.

Consequently, numerous studies have been carried out in these media for several years, giving rise to certain mathematically complex techniques such as stellar interferometry, inverse scattering, or fluorescence, among many others, trying to solve this problem. Regarding fluorescence, it is worth mentioning a test performed at the end of the 20th century, where a technique to improve the image quality of an object hidden by a diffuse medium combining fluorescence and absorption was tested, in it was shown that the image quality could be further improved by absorption, selecting the spectral range of the fluorescence light that is highly absorbed by the medium [3]. In addition, at the end of the 20th century, a new technique, simpler to perform, was introduced to improve vision through a random medium with high diffusion by using the absorption present in the medium. It was proven that absorption reduces the intensity of scattered light, that generates the image noise, below the intensity of the ballistic signal, which forms the image. This reduction in the signal-to-noise ratio allows to see through a diffusive medium that would be opaque without the presence of absorption [4]. Another test at this time showed that by using the absorption method to improve image quality in turbid media, the received energy decreases, but so does the path of the photons arriving at the detector, meaning that more scattered photons are absorbed, with a higher trajectory, than ballistic photons. In addition, it showed that the results obtained were similar to those achieved with the time-gating technique, which is more complex and expensive. This method is the most widely used for breast imaging. This last trial was performed to contemplate a new technique in medicine to detect breast tumors [5]. Gradually, the applications of this methodology have grown, reaching the military industry [6], and the astronomy [7].

The basic methodology we have used is similar that developed in [1]. In this work, the improvement of image quality is studied using black carbon powder as an absorber in two different scattering media, one consisting of zinc oxide nanoparticles, and the other of polystyrene nanoparticles. This last technique is the one of interest in the present investigation and on which the study has been based. For this purpose, we have made a series of samples and tested them in the labo-

ratory for subsequent analysis in Matlab using the SSIM function. In 2018 another paper was published following the research line of the 2016 [2]. In this article the influence of the wavelength of the incident light on the image enhancement is studied. Due to the angular distribution of the scattering depends on the size of the scatterers with respect to the wavelength of the incident light, they determine a new approach to image enhancement, selecting the appropriate wavelength range [2]. The most recent paper we have found is from 2019, in which authors analyze the absorption-scattering coupling and its impact on haze in random media. They also introduce the haze-absorption sensitivity spectrum which quantifies the capacity of absorption-induced haze supression [8].

It is also worth mentioning other interesting papers about absorption, scattering and turbid media, using other techniques and approaches [9–19].

Taking into account the aforementioned investigations, the aim of this paper is to compare the image enhancement achieved by graphene and black carbon powder as absorbers, and to study the influence of incident light by performing the experiments using white and red light.

2 Theory

To understand the absorption phenomenon, light must be understood as a corpuscle, quantized, with discrete values of energy. Absorption occurs when an electron is excited by a photon. Electrons occupy orbitals separated from each other by discrete amounsts of energy, in which the number of electrons is limited by the Pauli exclusion principle. When excited, the electron will move to a higher energy level, absorbing the energy and leaving a hole in its original position.

Imaging through absorbers leads to a loss of brightness since not all ballistic photons reach the detector. In the context of the image vision, scattering occurs, for instance, when a particulate system is interposed between the object and the detection system, such as turbid media. The rays emitted by the object are obstructed by the particles in the medium, deflecting their path.

Scattering depends on the particle size. We can distinguish two models within the context of our work: the Rayleigh and the Mie regimes.

When the particle size is much smaller than the wavelength of the incident light, we are in the Rayleigh case, while if the particle diameter is of the order or larger than the wavelength of the incident light, it is Mie scattering.

Imaging through scatterers generates a loss of quality of the trasmitted image, since the scatterers deflect the photons that arrive disorderly at the detector, resulting in blurred images. Therefore, in turbid media we can distinguish three types of photons: the ballistic photons that form the image, arriving in an orderly manner at the detector; the scattered photons, which generate blurred images because their trajectory has been altered and they arrive randomly at the camera; and the absorbed photons, which do not reach the detector, causing a loss of intensity.

3 Methodology

The procedure we have followed to perform the experiments its shown in the diagram below 2.

It has consisted of, first of all, the preparation of the samples, in which we have used graphene and black carbon powder as absorbers (both separately), polystyrene nanospheres as diffusers and distilled water as the matrix medium. We tested four different solutions, gradually increasing the amount of diffuser, with concentrations of 30, 50, 70 and 100 µl in 10 ml of distilled water, and absorbers concentrations of 0.3; 0.4; 0.5; 0.6; 0.7; 0.8; 1.3 and 3.3 mg for the first three solutions and 0.5 and 1.3 for the last one.

Afterwards, we introduce the samples into the cuvette of the optical system for imaging. The imaging setup we use consisted of a CMOS camera, a 1951 US Air Force resolution target as the object, a biconvex convergent type lens, a rectangular glass cuvette to place the samples in between the camera and the object. As radiation source, we used an incoherent white led light with a 650 nm bandpass filter, and without.

Once the images have been taken, to compare and evaluate their quality, first, we must select those that are comparable with each other, for what we use the signal-to-noise ratio following three different methods depending on the application. To calculate the signal-to-noise ratio

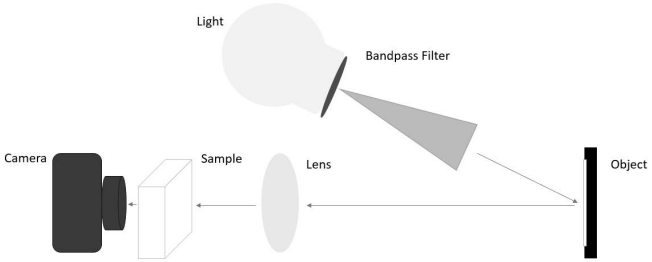

Figure 1: Imaging setup.

of the images we use the following formula:

$$SNR = \frac{\prec I \succ}{\sqrt{\prec I^2 \succ - \prec I \succ^2}}$$

Where, $I =$ Image intensity and $\prec I \succ =$ Average image intensity

Here, we present the methods we have used to choose the images based on the application. The resulst vary depending on the method selected.

Method 1: We select the images considering the signal-to-noise ratio of the reference image. This criterion is useful for those applications where the reference image is known, for example, in the geostationary satellite case.

Method 2: Considering the exposure time of the reference image we select the disturbed one and, depending on its signal-to-noise ratio, we choose the images with an absorber. This criterion is useful for images whose damage degree is such that it is not possible to return to the reference one, and therefore, it is necessary to work on the disturbed image. For instance, in optical space elements that have suffered such a deterioration that you cannot return to their initial conditions, and therefore it is required to work with the deteriorated image.

Method 3: Considering the exposure time of the reference image we select the same disturbed one. Then, to select the images with an absorber we vary the exposure time seeking to return to the signal-to-noise ratio conditions of the reference. This criterion is useful for

applications like method 1 but when the disturbance appears instantaneously.

Once we have selected the images to evaluate them we use the structural similarity index (SSIM) in Matlab.

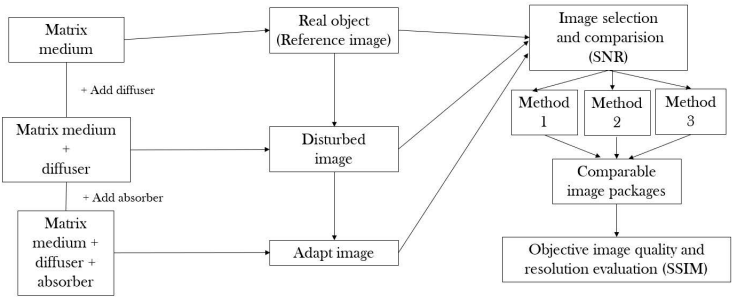

Figure 2: Procedure diagram.

SSIM quantifies the similarity of an image regarding the reference one, taking into consideration the structure, contrast, and illuminance of the images (x,y), as we can see below [20,21].

1) Iluminance comparison:

$$l(x,y) = \frac{2\mu_x\mu_y + C_1}{\mu_x^2 + \mu_y^2 + C_1},$$

where $C_1 = (0,01 \cdot 2^{bitsperpixel} - 1)^2$

2) Contrast comparison:

$$c(x,y) = \frac{2\sigma_x\sigma_y + C_2}{\sigma_x^2 + \sigma_y^2 + C_2},$$

being $C_2 = (0,03 \cdot 2^{bitsperpixel} - 1)^2$.

3) Structure comparison:

$$s(x,y) = \frac{\sigma_{xy} + C_3}{\sigma_x\sigma_y + C_3}$$

Here, $\mu_x, \mu_y, \sigma_x, \sigma_y$ and σ_{xy} are the local means, standard deviations and cross-covariance. From these quantities may be demonstrated that the SSIM index is:

$$SSIM(x,y) = \frac{(2\mu_x\mu_y + C_1)(2\sigma_{xy} + C_2)}{(\mu_x^2 + \mu_y^2 + C_1)(\sigma_x^2 + \sigma_y^2 + C_2)}$$

4 Experimental results

In this section we show the most important results obtained. We have compiled those experiments in which an improvement of graphene over graphite is detected, for each method explained above with red and white light sources. First we show the results for red light for each technique, and then those obtained with white light.

As we can observe, both numerically by means of SSIM and visually, the fourth image on the right, adapted with graphene, is the one that most resembles the reference picture, improving with respect to the image perturbed with the diffuser and the image adapted with graphite (Figures 3 to 8).

For the image series from 3 to 5 with red light we observe that the SSIM values achieved for the adapted versus perturbed images present larger differences than for the white light case (Figures 6 to 8), especially for method 1.

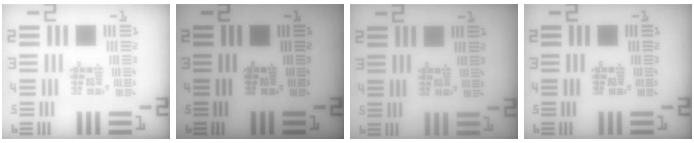

(a) **(b)** **(c)** **(d)**

Figure 3: Results of the method 1 for red light. (a) Reference image 10ml distilled water. (b) Disturbed image 30 μl polystyrene, SSIM=0.5497. (c) Image with 0.4 mg graphite, SSIM=0.6818. (d) Image with 0.4 mg graphene, SSIM=0.7849.

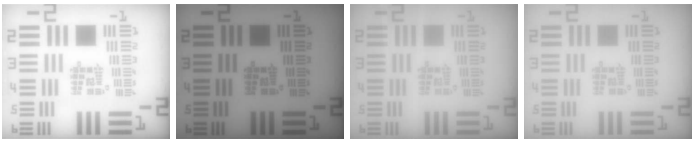

(a) (b) (c) (d)

Figure 4: Results of the method 2 for red light. (a) Reference image 10ml distilled water. (b) Disturbed image 50 μl polystyrene, SSIM=0.4105. (c) Image with 3.3 mg graphite, SSIM=0.6629. (d) Image with 3.3 mg graphene, SSIM=0.7107.

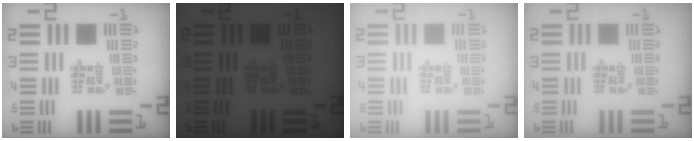

(a) (b) (c) (d)

Figure 5: Results of the method 3 for red light. (a) Reference image 10ml distilled water. (b) Disturbed image 70 μl polystyrene, SSIM=0.5868. (c) Image with 0.4 mg graphite, SSIM=0.9717. (d) Image with 0.4 mg graphene, SSIM=0.9968.

The results obtained using white light for the three methods are shown below.

(a) (b) (c) (d)

Figure 6: Results of the method 1 for white light. (a) Reference image 10ml distilled water. (b) Disturbed image 70 μl polystyrene, SSIM= 0.9762. (c)Image with 0,6 mg graphite, SSIM=0.9918. (d) Image with 0.6 mg graphene, SSIM=0.9920.

(a) (b) (c) (d)

Figure 7: Results of the method 2 for white light. (a) Reference image 10ml distilled water. (b) Disturbed image 50 μl polystyrene, SSIM= 0.5815. (c) Image with 3.3 mg graphite, SSIM=0.7384. (d) Image with 3.3 mg graphene, SSIM=0.7736.

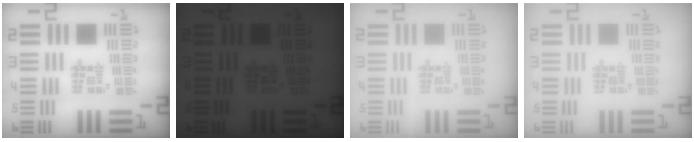

(a) (b) (c) (d)

Figure 8: Results of the method 3 for white light. (a) Reference image 10ml distilled water. (b) Disturbed image 70 μl polystyrene, SSIM= 0.4525. (c) Image with 0.6 mg graphite, SSIM=0.9918. (d) Image with 0.6 mg graphene, SSIM=0.9920.

5 Conclusion

In this paper we have presented the image enhancement by the absorption technique using graphene as an absorber. Likewise, a comparison between the enhancement obtained by graphene and graphite, and white and red light, has been made.

We have found that, in most cases, for the type 2 suspension and red light, the concentration at which the best SSIM values are achieved for graphene is 0.4 mg. We have encountered that in the case of vision loss due to image intensity saturation, there is a generalized improvement when introducing both, polystyrene nanospheres and the two absorbers. We expected significant results in which the enhancement would be visible to the naked eye for any of the three methods, however, for method 1 the improvements are practically negligible, being visibly unnoticeable. Also, we found the most important results for method 3, and the least remarkable for method 1. We found more significant results with red light rather than with white light. In addition, white light saturates sooner.

References

1. M. Tanzid, N. J. Hogan, A. Sobhani, H. Robatjazi, A. K. Pediredla, A. Samaniego, A. Veeraraghavan, and N. J. Halas, "Absorption-induced image resolution enhancement in scattering media," *ACS Photonics*, vol. 3, no. 10, pp. 1787–1793, 2016.
2. M. Tanzid, N. J. Hogan, H. Robatjazi, A. Veeraraghavan, and N. J. Halas, "Absorption-enhanced imaging through scattering media using carbon black nano-particles: From visible to near infrared wavelengths," *Journal of Optics*, vol. 20, no. 5, p. 054001, 2018.
3. K. Yoo, Z.-W. Zang, S. A. Ahmed, and R. Alfano, "Imaging objects hidden in scattering media using a fluorescence–absorption technique," *Optics letters*, vol. 16, no. 16, pp. 1252–1254, 1991.
4. K. Yoo, F. Liu, and R. Alfano, "Imaging through a scattering wall using absorption," *Optics letters*, vol. 16, no. 14, pp. 1068–1070, 1991.
5. D. Contini, H. Liszka, A. Sassaroli, and G. Zaccanti, "Imaging of highly turbid media by the absorption method," *Applied optics*, vol. 35, no. 13, pp. 2315–2324, 1996.

6. P. B. Schwering, R. A. Kemp, and K. Schutte, "Image enhancement technology research for army applications," in *Infrared Imaging Systems: Design, Analysis, Modeling, and Testing XXIV*, vol. 8706. SPIE, 2013, pp. 198–208.
7. R. Tyson, "Principles of adaptive optics third edition," 2010.
8. L. Zhao, M. Blackman, L. Zhang, B. Bhatia, A. Leroy, E. Strobach, and E. N. Wang, "Plasmonic absorption-induced haze suppression in random scattering media," *Applied Physics Letters*, vol. 114, no. 25, p. 251102, 2019.
9. J. J. Dolne, K. M. Yoo, F. Liu, and R. R. Alfano, "Continuous wave near infrared fourier space and absorption imaging through random scattering media," in *Advances in Laser and Light Spectroscopy to Diagnose Cancer and Other Diseases*, vol. 2135. SPIE, 1994, pp. 209–212.
10. S. F. Liew, S. M. Popoff, A. P. Mosk, W. L. Vos, and H. Cao, "Transmission channels for light in absorbing random media: from diffusive to ballistic-like transport," *Physical Review B*, vol. 89, no. 22, p. 224202, 2014.
11. S. F. Liew and H. Cao, "Modification of light transmission channels by inhomogeneous absorption in random media," *Optics express*, vol. 23, no. 9, pp. 11 043–11 053, 2015.
12. M. Tanzid, A. Sobhani, C. J. DeSantis, Y. Cui, N. J. Hogan, A. Samaniego, A. Veeraraghavan, and N. J. Halas, "Imaging through plasmonic nanoparticles," *Proceedings of the National Academy of Sciences*, vol. 113, no. 20, pp. 5558–5563, 2016.
13. X. L. Deán-Ben, H. Estrada, A. Özbek, and D. Razansky, "Controlling the light distribution through turbid media with wavefront shaping based on volumetric optoacoustic feedback," in *Adaptive Optics and Wavefront Control for Biological Systems II*, vol. 9717. SPIE, 2016, pp. 198–202.
14. J. A. Carr, M. Aellen, D. Franke, P. T. So, O. T. Bruns, and M. G. Bawendi, "Absorption by water increases fluorescence image contrast of biological tissue in the shortwave infrared," *Proceedings of the National Academy of Sciences*, vol. 115, no. 37, pp. 9080–9085, 2018.
15. M. I. Mishchenko, L. Liu, and J. W. Hovenier, "Effects of absorption on multiple scattering by random particulate media: exact results," *Optics express*, vol. 15, no. 20, pp. 13 182–13 187, 2007.
16. S. A. Ahmed, Z.-W. Zang, K. M. Yoo, M. Ali, and R. Alfano, "Effect of multiple light scattering and self-absorption on the fluorescence and excitation spectra of dyes in random media," *Applied optics*, vol. 33, no. 13, pp. 2746–2750, 1994.
17. W. Liu, Z. Zhou, L. Chen, X. Luo, Y. Liu, X. Chen, and W. Wan, "Imaging through dynamical scattering media by two-photon absorption detectors," *Optics Express*, vol. 29, no. 19, pp. 29 972–29 981, 2021.

18. M. K. Swami, S. Manhas, H. Patel, and P. K. Gupta, "Mueller matrix measurements on absorbing turbid medium," *Applied Optics*, vol. 49, no. 18, pp. 3458–3464, 2010.

19. Z. Feng, T. Tang, T. Wu, X. Yu, Y. Zhang, M. Wang, J. Zheng, Y. Ying, S. Chen, J. Zhou *et al.*, "Perfecting and extending the near-infrared imaging window," *Light: Science & Applications*, vol. 10, no. 1, pp. 1–18, 2021.

20. Z. Wang, A. C. Bovik, H. R. Sheikh, and E. P. Simoncelli, "Image quality assessment: from error visibility to structural similarity," *IEEE transactions on image processing*, vol. 13, no. 4, pp. 600–612, 2004.

21. A. Hore and D. Ziou, "Image quality metrics: Psnr vs. ssim," in *2010 20th international conference on pattern recognition*. IEEE, 2010, pp. 2366–2369.